ISSN 1063-7834, Physics of the Solid State, 2020, Vol. 62, No. 11, pp. 2058–2062. © Pleiades Publishing, Ltd., 2020.
Russian Text © The Author(s), 2020, published in Fizika Tverdogo Tela, 2020, Vol. 62, No. 11, pp. 1835–1839.

DIELECTRICS

Tolerance Factor for Huntite-Family Compounds

M. S. Molokeev[a, b, *] and S. O. Kuznetsov[a]

[a] *Siberian Federal University, Krasnoyarsk, 660041 Russia*

[b] *Kirensky Institute of Physics, Krasnoyarsk Scientific Center, Siberian Branch, Russian Academy of Sciences, Krasnoyarsk, 660036 Russia*

**e-mail: msmolokeev@mail.ru*

Received June 3, 2020; revised June 3, 2020; accepted June 26, 2020

Abstract—85 $RM_3(BO_3)_4$ (R is the rare-earth element (Y, La–Lu) and M = Al, Sc, Cr, Fe, or Ga) compounds with the huntite structure have been analyzed. The analysis of the structures has made it possible to determine critical atomic displacements during the phase transition $R32 \leftrightarrow P3_121$ and establish how these critical displacements can be controlled by varying the ionic radii. A tolerance factor has been derived and its threshold value below which the structure is stable in the $R32$ phase and above it, in the distorted $P3_121$ phase, has been found. The formula has been tested on more than 30 huntite-family compounds and good agreement has been obtained. Therefore, it can be used with confidence to predict new compounds. At the moment, the tolerance factor has allowed us to establish previously unknown regularities in huntites.

Keywords: huntites, tolerance factor, phase transition, structural stability, crystal structure

DOI: 10.1134/S1063783420110190

1. INTRODUCTION

In the last few decades, borate crystals have evoked a great interest due to a wide variety of their structures [1]. Borates are optically transparent in a wide spectral range and have the high chemical and mechanical stability. Borates with a huntite structure ($CaMg_3(CO_3)_4$ huntite, sp. gr. $R32$) attract close attention by their valuable magnetoelectric [2, 3] and spectroscopic [4–6] properties promising for engineering applications. The general formula of the huntite-family borates is $RM_3(BO_3)_4$, where R is the rare-earth element (Y, La–Lu) and M is Al, Sc, Cr, Fe, or Ga.

The $RM_3(BO_3)_4$ crystal structure type depends on chemical composition and crystallization conditions (Table 1). In each structure, three types of coordination polyhedra are distinguished: trigonal prisms RO_6, octahedra MO_6, and polyhedra BO_3 in the form of triangles. In the most wide-spread phase with the R32 symmetry, there is one RO_6, one MO_6, and two BO_3 in the independent part of the cell (Fig. 1). Along with the $R32$ phase, the trigonal $P3_121$ and $P321$ and monoclinic $C2/c$, Cc, and $C2$ phases have been noted. However, for huntites, no quantitative measure has been proposed yet that would allow one to estimate the formation of a desired phase and make a quick symmetry forecast. Such a measure, as a rule, is the tolerance factor, which is an indicator of the stability and distortion of crystal structures [7]. Initially, it was only used to describe the perovskite structure [8], but, at present, the tolerance factors are used also, e.g., for ilmenite [9], garnets [10], pyrochlores [11], and chalcogenides with the general formula $ABCX_3$ [12].

In this work, we propose a tolerance factor for determining the stability of the $R32$ phase of huntite-like crystals and its threshold value corresponding to the transition to the $P3_121$ phase. The derived formula can be used to predict the phase symmetry and, consequently, some properties of a substance, using only the assumed chemical formula.

2. EXPERIMENTAL

To establish the regularities of the formation of different huntite phases, it was decided to collect data on

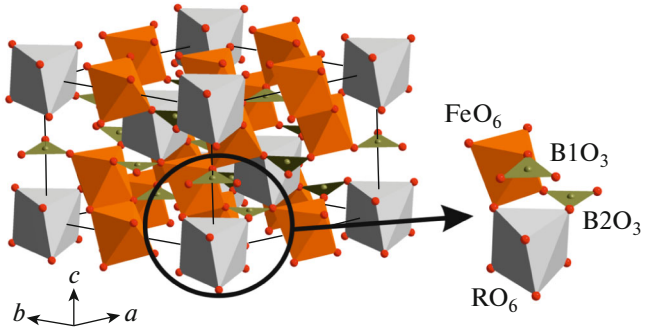

Fig. 1. Crystal structure of the $RM_3(BO_3)_4$ compound in the $R32$ phase. The independent part of the cell is outlined with a circle.

Table 1. List of basic huntite compounds with the general chemical formula $LnM(BO_3)_4$ from the COD and ICSD databases (the compounds are sorted ascending the tolerance factor (*t* factor) and classified by space groups)

Sp. gr.	Ln	M	*IR* Ln, Å	*IR* Me, Å	*t* factor
*R*32	Nd	Al	1.109	0.535	1.603
*R*32	Eu	Al	1.066	0.535	1.633
*R*32	Gd	Al	1.053	0.535	1.642
*R*32	La	Fe	1.160	0.645	1.644
*R*32	Nd	Ga	1.109	0.620	1.663
*R*32	Y	Al	1.019	0.535	1.666
*R*32	Ho	Al	1.015	0.535	1.669
*R*32	Er	Al	1.004	0.535	1.677
*R*32	Nd	Fe	1.109	0.645	1.680
*R*32	Tm	Al	0.994	0.535	1.684
*R*32	Eu	Cr	1.066	0.615	1.689
*R*32	Yb	Al	0.985	0.535	1.690
*R*32	$Y_{0.5}Bi_{0.5}$	Fe	1.095	0.645	1.690
*R*32	Gd	Cr	1.053	0.615	1.699
*R*32	Sm	Fe	1.079	0.645	1.701
*R*32	La	Sc	1.160	0.745	1.715
*R*32	Gd	Fe	1.053	0.645	1.720
*R*32	Ce	Sc	1.143	0.745	1.727
*R*32	Tb	Fe	1.040	0.645	1.729
*R*32	Er	Cr	1.004	0.615	1.733
*R*32	Er	Fe	1.004	0.645	1.754
$P3_121$	$Y_{0.94}Bi_{0.06}$	Fe	1.028	0.645	1.737
$P3_121$	Dy	Fe	1.027	0.645	1.738
$P3_121$	$Ho_{0.963}Bi_{0.037}$	Fe	1.021	0.645	1.742
$P3_121$	Nd	Sc	1.109	0.745	1.751

their possible structures from the COD (http://www.crystallography.net/cod/) and ICSD databases. About 85 structures were found at different synthesis and shooting temperatures. All the phases can be roughly divided into trigonal (*R*32, $P3_121$, and *P*321) and monoclinic (*C*2/*c*, *Cc*, and *C*2). The monoclinic phases are significantly different from the trigonal ones in their structure and properties [13] and were not considered in this work. Recent investigations [14] showed that the *P*321 phase observed previously in $NdSc_3(BO_3)_4$ is most likely erroneous and the more correct model $P3_121$ was chosen for it. Therefore, the *R*32 and $P3_121$ phases were of particular interest, since they cover most of the stored structures. In addition, it should be noted that the phase transition $R32 \leftrightarrow P3_121$ can occur both in temperature and in composition, which was reported earlier in [15–18]; therefore, it is especially interesting to derive the tolerance factor for these particular phases. In this work, the trigonal phases *R*32 and $P3_121$ (see Table 1) were studied under normal conditions. Here, we did not consider the symmetry changes with temperature, since the tolerance factor suggests the effect of only geometric characteristics on symmetry and our goal was to establish the regularities only for the $RM_3(BO_3)_4$ composition. It should be noted that the dependence of the temperature of the phase transition $R32 \leftrightarrow P3_121$ on ionic radii has been already studied [15] and the conclusion about the linear dependence $T = A \times IR(R) + B$ has been made, where *A* and *B* are the coefficients and *IR*(R) is the ionic radius of a rare-earth element (Y, La–Lu), which was confirmed in part in [16].

To establish the regularities of the transformation of *R*32 into $P3_121$, we thoroughly compared the $TbFe_3(BO_3)_4$ structures in the *R*32 (300 K) and $P3_121$ (2 K) phases [18] using the ISODISTORT software [19]. It was found that, during the phase transition, the boron triangle $B1O_3$ and the prism TbO_6 do not undergo any particular changes. However, the $B2O_3$ triangle splits into two positions, $B2O_3$ and $B3O_3$, and the FeO_6 octahedron also splits into two positions, $Fe1O_6$ and $Fe2O_6$. According to the ISODISTORT analysis of distortion modes, the largest displacement in the structure is experienced by the O_2 atom belonging to the $B2O_3$ boron triangle (Fig. 2). It is this critical displacement that leads to the symmetry change.

The O2 atom is located in a cavity bounded by the Fe2–O2–B2–O7–Tb–O3–B2–O7–Tb–O4 atoms (Fig. 2). It was assumed that the size of this cavity in the direction of the greatest displacement of the O2 atom (Fig. 2) affects the stability of the *R*32 phase. If the cavity is small, then it is difficult for the O2 atom to move; therefore, there are no critical displacement and phase change in $P3_121$; i.e., the *R*32 phase is retained. If the cavity is large, then the O2 atom is easily displaced in the arrow direction and the *R*32 phase passes to $P3_121$.

It was decided to calculate the size of this cavity using the data on the radii of ions forming the structure. It can be seen in Fig. 3 that this cavity is equal to the difference between the length of the upper row of ions

$$L1 = IR(B) + 2 \times IR(O) + 2 \times IR(M) + IR(O) + IR(B) \quad (1)$$

and two ionic radii of ion R: $2 \times L2 = 2 \times IR(R)$. The ratio between the difference $L1 - 2 \times L2$ and the oxygen ion size $L3 = 2 \times IR(O)$ is a tolerance factor that determines the symmetry of the huntite phase for any composition:

$$t = \frac{L1 - 2 \times L2}{L3}. \quad (2)$$

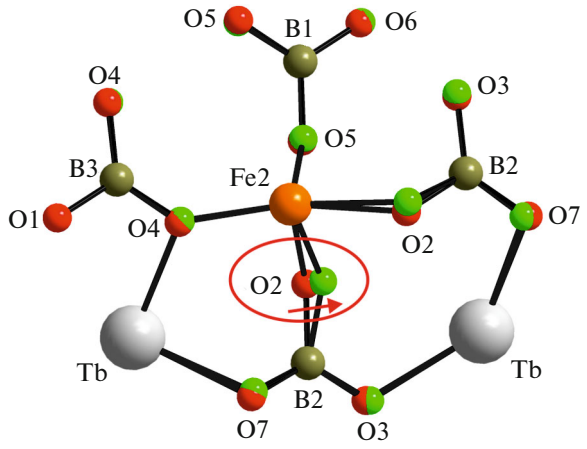

Fig. 2. Change in the $TbFe_3(BO_3)_4$ structure during the phase transition from $R32$ (300 K) to $P3_121$ (2 K). The O2 atom undergoing the largest displacement during the phase transition is outlined with a circle. The direction of displacement upon cooling is shown by an arrow.

Substituting Eq. (1) into (2) and making simplifications, we arrive at

$$t = \frac{IR(\mathrm{B}+2)\times IR(\mathrm{O}) + IR(\mathrm{M}) - IR(\mathrm{R})}{IR(\mathrm{O})}, \qquad (3)$$

where $IR(\mathrm{O}) = IR(\mathrm{O}^{2-}, \mathrm{CN} = 6) = 1.42$ Å is the oxygen ionic radius, $IR(\mathrm{B}) = IR(\mathrm{B}^{+3}, \mathrm{CN} = 3) = 0.01$ Å is the boron ionic radius, $IR(\mathrm{M}) = IR(\mathrm{M}^{3+}, \mathrm{CN} = 6) = 0.6$–$0.75$ (Å) is the radius of a metal ion, $IR(\mathrm{R}) = IR(\mathrm{Ln}^{3+}, \mathrm{CN} = 8) = 0.8 - 1.7$ (Å) is the radius of a rare-earth ion, and CN is the coordination number for a specific ion. In this work, the coordination number CN = 8 is used for the rare-earth ions R, since, along with six nearest oxygen atoms with a distance of d(Ln–O) ~ 2.4 Å, there are two more oxygen atoms with a distance of d(Ln–O) ~ 2.8 Å. As a result, the polyhedron has the form of a two-cap trigonal prism. The Shannon ionic radii were used [20].

3. RESULTS

For all the investigated compounds, the tolerance factor was calculated using formula (3) and the substances were sorted in Table 1 according to this t value from the minimum to the maximum. The sorting divided the groups of trigonal phases into two subclasses with a threshold tolerance factor of $t_0 = 1.737$. The factor smaller than this value leads to the $R32$ phase. The factor larger than this value leads to the $P3_121$ phase, except for the $ErFe_3(BO_3)_4$ ($R32$) compound, which has an anomalously large factor (1.754). This point (Fig. 4) can be a random outburst and, either this crystal has different chemical composition or the phase is actually $P3_121$ rather than $R32$. Most of the compounds are easily divided into two subclasses and we can assume that the formula for the tolerance

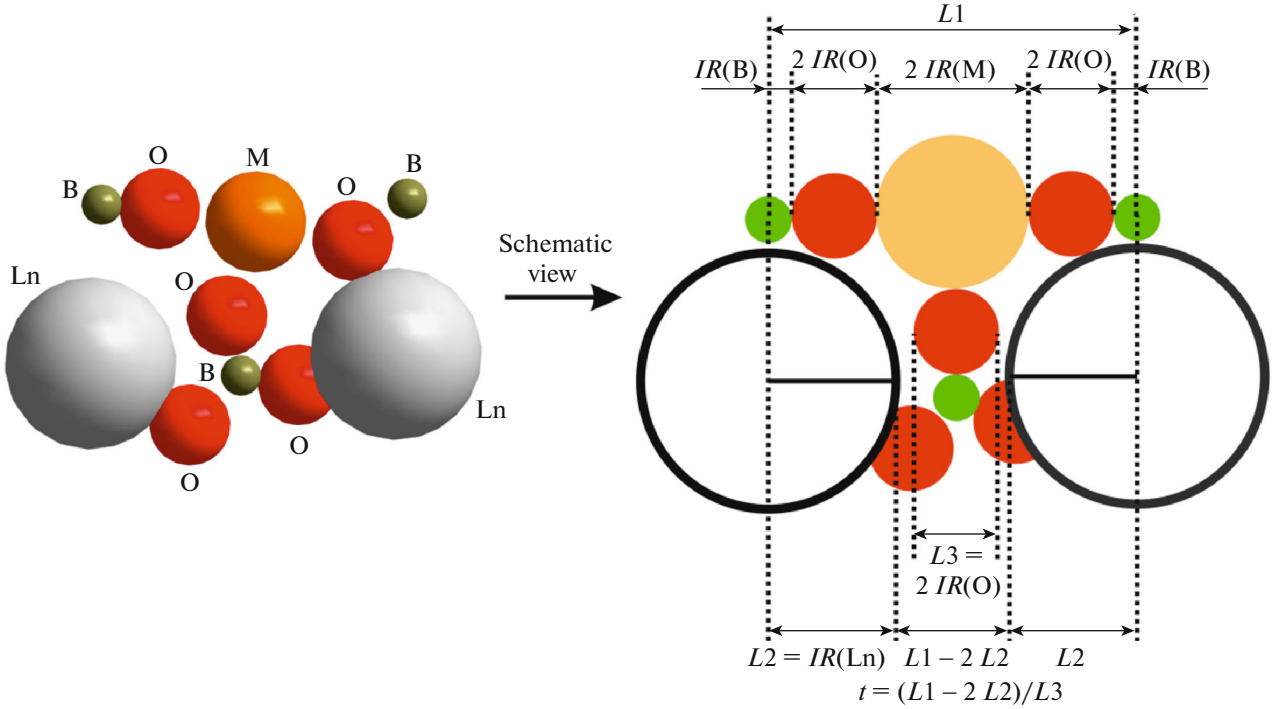

Fig. 3. (a) Coordination environment of the boron triangle BO_3 in $RM_3(BO_3)_4$. Ions R^{3+}, M^{3+}, B^{3+}, and O2 are shown by spheres with the radii similar to ionic radii. (b) Characteristic ion sizes and main lengths used in the calculation of the tolerance factor t.

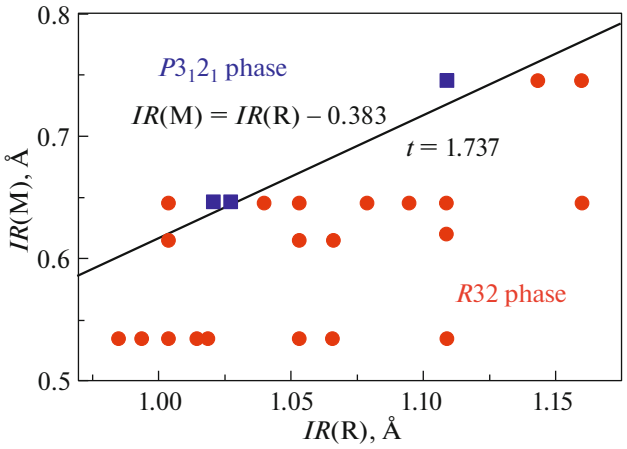

Fig. 4. Diagram of the distribution of the $R32$ (circles) and $P3_121$ (squares) phases of the available $RM_3(BO_3)_4$ compounds over the ionic radii $IR(M)$ and $IR(R)$. The oblique line characterizes the boundary compounds with a tolerance factor of $t = 1.737$. All the compounds below this line are in the $R32$ phase and those above it, in the $P3_121$ phase. Only one circle is located beyond its zone, which can be an outburst.

factor does contain data on the stability region of the $R32$ phase.

Analysis of formula (3) shows the existing difference between the contributions of M and R ions to the stability of the $R32$ phase in the $RM_3(BO_3)_4$ compounds. First, an increase in the R ionic radius reduces the tolerance factor and leads to the $R32$ phase, while an increase in the M ionic radius, on the contrary, increases the probability of implementation of the distorted $P3_121$ phase. Second, $IR(M)$ and $IR(R)$ have different ranges: $IR(M)$ is within 0.6–0.75 (Å) and the ionic radius of all the possible R ions ranges between 0.8–1.25 (Å) (Table 1). Consequently, the R ion makes a greater contribution to the tolerance factor t and affects more strongly the stability of the $R32$ phase.

Using this knowledge, one can immediately predict that the compounds with R = La, Pr, Nd, Pm, Sm, and Eu will most likely be in the $R32$ phase, since, at any known M values, the tolerance factor will be smaller than 1.737. This can easily be confirmed by calculating the tolerance factor for some compounds that have not been obtained in real experiments yet. As an example, let us consider the compounds with the chemical compositions $PrFe_3(BO_3)_4$ and $LaAl_3(BO_3)_4$ and use the ionic radii $IR(Pr) = 1.126$ Å, $IR(Fe) = 0.645$ Å, $IR(La) = 1.16$ Å, and $IR(Al) = 0.535$ Å. As a result, we obtain $t(PrFe_3(BO_3)_4 = 1.668$ and $t(LaAl_3(BO_3)_4 = 1.567$, which is much lower than a threshold value of $t_0 = 1.737$ and these compounds will most likely exist in the $R32$ phase under normal conditions. It should be noted that, for the huntite $CaMg_3(CO_3)_4$ ($IR(Ca) = 1.12$ Å, $IR(Mg) = 0.72$ Å, $IR(C) = -0.08$ Å, and $IR(O) = 1.42$ Å) the tolerance factor is $t = 1.662$; therefore, the huntite should exist in the $R32$ phase, which is actually the case. Hence, the formula is most likely applicable not only to borates, but also to other compounds with different composition.

4. CONCLUSIONS

By now, a great number of huntites $RM_3(BO_3)_4$ have been discovered, but, until recently, there has been a lack of clear understanding of the mechanism of $R32$ phase stabilization and the processes leading to the structural distortion. In this work, it was found that the rotation of only one boron triangle BO_3 of the two and, consequently, the displacement of one oxygen atom is the most critical and leads to the phase transition $R32 \leftrightarrow P3_121$. Understanding of this fact allowed us to derive a formula for the tolerance factor $t = \dfrac{IR(B+2)\times IR(O) + IR(M) - IR(R)}{IR(O)}$, which significantly contributes to further investigations and prediction of the structures of huntite-family compounds.

The tolerance factor for the available huntite-family compounds was calculated and its threshold value $t_0 = 1.737$ was determined. All the tolerance factors higher than this threshold will correspond to the $P3_121$ phase. All the tolerance factors below 1.737 form the stability region of the $R32$ phase.

It was established from the formula for the tolerance factor that the larger the ionic radius of the rare-earth element R and the smaller the ionic radius of the metal M, the more probable the $R32$ phase. Vice versa, the smaller the R ionic radius and the larger the M one, the higher the probability of existence of the distorted $P3_121$ phase under normal conditions.

The prediction of the t factor describes well the phase separation of the compounds by symmetries, as can be seen in Table 1 and Fig. 1. Therefore, this formula can be used with confidence to predict new compounds.

CONFLICT OF INTEREST

The authors declare that they have no conflicts of interest.

REFERENCES

1. D. Xue, K. Betzler, H. Hesse, and D. Lammers, Solid State Commun. **114**, 21 (2000).
2. J. A. Campá, C. Cascales, E. Gutiérrez-Puebla, M. A. Monge, I. Rasines, and C. Ruíz-Valero, Chem. Mater. **9**, 237 (1997).
3. K.-C. Liang, R. P. Chaudhury, B. Lorenz, Y. Y. Sun, L. N. Bezmaternykh, V. L. Temerov, and C. W. Chu, Phys. Rev. B **83**, 180417 (2011).

4. J.-P. Meyn, T. Jensen, and G. Huber, IEEE J. Quantum Electron. **30**, 913 (1994).
5. I. Couwenberg, K. Binnemans, H. de Leebeeck, and C. Görller-Walrand, J. Alloys Compd. **274**, 157 (1998).
6. D. A. Ikonnikov, A. V. Malakhovskii, A. L. Sukhachev, V. L. Temerov, A. S. Krylov, A. F. Bovina, and A. S. Aleksandrovsky, Opt. Mater. **37**, 257 (2014).
7. H. Kronmüller and S. Parkin, in *Handbook of Magnetism and Advanced Magnetic Materials* (Wiley, New York, 2007), Vol. 1.
8. V. M. Goldschmidt, Naturwissensch. **14**, 477 (1926).
9. X. Liu, R. Hong, and C. Tian, J. Mater. Sci.: Mater. Electron. **20**, 323 (2009).
10. Z. Song, D. Zhou, and Q. Liu, Acta Crystallogr., C **75**, 1353 (2019).
11. R. Mouta, R. X. Silva, and C. W. A. Paschoal, Acta Crystallogr., B **69**, 439 (2013).
12. N. O. Azarapin, A. S. Aleksandrovsky, V. V. Atuchin, T. A. Gavrilova, A. S. Krylov, M. S. Molokeev, Sh. Mukherjee, A. S. Oreshonkov, and O. V. Andreev, J. Alloys Compd. **832**, 153134 (2020).
13. A. S. Oreshonkov, E. M. Roginskii, N. P. Shestakov, I. A. Gudim, V. L. Temerov, I. V. Nemtsev, M. S. Molokeev, S. V. Adichtchev, A. M. Pugachev, and Y. G. Denisenko, Materials **13**, 545 (2020).
14. E. V. Eremin, M. S. Pavlovskiy, I. A. Gudim, V. Temerov, M. Molokeev, N. D. Andryushin, and E. V. Bogdanov, J. Alloys Compd. **828**, 154355 (2020).
15. Y. Hinatsu, Y. Doi, K. Ito, M. Wakeshima, and A. Alemi, J. Solid State Chem. **172**, 438 (2003).
16. E. Moshkina, S. Krylova. I Gudim, M. Molokeev, V. Temerov, M. Pavlovskiy, A. Vtyurin, and A. Krylov, Cryst. Growth Des. **20**, 1058 (2020).
17. M. S. Pavlovskii and N. D. Andryushin, Phys. Solid State **61**, 2049 (2019).
18. S. A. Klimin, A. B. Kuzmenko, M. A. Kashchenko, and M. N. Popova, Phys. Rev. B **93**, 054304 (2016).
19. H. T. Stokes, D. M. Hatch, B. J. Campbell, and D. E. Tanner, J. Appl. Crystallogr. **39**, 607 (2006).
20. R. D. Shannon, Acta Crystallogr., A **32**, 751 (1976).

Translated by E. Bondareva